Comparative Analysis of Tunable Dual Split Ring Resonator in Different Dimensional Configurations

Author

Muhammad Shoaib

Reg. Number

00000148518

Supervisor

Dr. Muhammad Naveed

DEPARTMENT OF ELECTRICAL ENGINEERING

COLLEGE OF ELECTRICAL & MECHANICAL ENGINEERING

NATIONAL UNIVERSITY OF SCIENCES AND TECHNOLOGY

ISLAMABAD

Comparative Analysis of Tunable Dual Split Ring Resonators in Different Dimensional Configurations

Author

Muhammad Shoaib

Reg. Number

00000148518

A thesis submitted in partial fulfillment of the requirements for the degree of

MS Electrical Engineering

Thesis Supervisor:

Dr. Muhammad Naveed

Thesis Supervisor's Signature: _____

DEPARTMENT OF ELECTRICAL ENGINEERING

COLLEGE OF ELECTRICAL & MECHANICAL ENGINEERING

NATIONAL UNIVERSITY OF SCIENCES AND TECHNOLOGY

ISLAMABAD

DECLARATION

I certify that this research work titled "**Comparative Analysis of Tunable Dual Split Ring Resonators in Different Dimensional Configurations"** is my own work. The work has not been submitted elsewhere for assessment. The material used from other sources, has been properly acknowledged / referred.

Signature of Student
Muhammad Shoaib
Reg No. 00000148518

LANGUAGE CORRECTNESS CERTIFICATE

This thesis has been read by an English expert and is free of typing syntax, semantic, grammatical and spelling mistakes. Thesis is also according to the format given by the university.

Signature of Student
Muhammad Shoaib
Reg No. 00000148518

Signature of Supervisor

COPYRIGHT STATEMENT

ACKNOWLEDGMENT

First and foremost, I am thankful to **ALLAH** for His countless blessings and for giving me the strength and courage to undertake this novel project and see to its outcomes. I am also thankful for the tremendous support, courage and prayers of my parents and family members. I wish to record my deepest obligation to my parents and my brother for their prayers, encouragement and financial as well as moral support during my studies.

I would also like to express my deep gratitude to **Dr. Muhammad Naveed**, my supervisor, for his guidance, support, encouragement and help in development of my ideas and research outcomes.

I am thankful to all my GEC Members **Dr. Syed Muhammad Tahir Zaidi** and **Dr. Mashood Ahmad** for their help and guidance. I am also very thankful to **Tahir Ejaz** for his continuous guidance during the research, support and unconditional help.

I also thank my friends especially **Malik Muhammad Haris Amir** for giving me their sincere and unconditional support whenever it was needed.

Dedicated to my parents, wife, children and siblings, whose profound support, enormous sacrifices and generous assistance led me to this achievement

ABSTRACT

A simulation based analysis has been carried out to find most appropriate and practical configuration of SSRs; Dual broadside coupled split ring resonators to provide a considerable shift in resonant frequency. This configuration has been optimized keeping in view the shift in resonant frequency and quality factor. Most suitable parameters have been found which provide maximum shift in resonant frequency and minimum variance in quality factor. An analytical solution has been proposed based on capacitor-inductor resonant network analogy to approximate the resonant frequency. Expressions for calculation of overall capacitance of dual split rings have been developed. Finally, calculated resonant frequencies from developed analytical solution have been compared with the simulated results.

TABLE OF CONTENTS

LIST OF TABLES

LIST OF FIGURES

CHAPTER 1

INTRODUCTION

INTRODUCTION

Split ring resonators in various configurations have become an important component for design at microwave frequencies. These components provide low phase noise, moderate quality factor and ease of fabrication, even at minute scales. High frequency circuits including filters, oscillators, frequency meters and tuned amplifiers can be designed with reduced size and cost. Recent advances in thin films processing have materialized these devices at nanometer levels. A split ring consists of a conductive cylindrical loop (ring) cut by one or more longitudinal slots. A typical split ring is shown in Figure 1.1a. Split rings can be fabricated in various geometrical configurations; commonly circular, square and rectangular with single / multiple rings and single / multiple slots. Figure 1.1b shows some typical geometries used for split rings. Most of the structures are resonant due to inherent capacitances and inductances.

Split ring resonators have vast applications areas which include microwave filters, oscillators, amplifiers, material characterization and analysis, magnetic resonance spectroscopy, magnetron amplifiers, micro sensors for pharmaceutical, clinical and electro-medical applications and meta-materials.

1.1. Motivation

The first and foremost motivation to conduct this research is presence of a large research group which is already working in this field in College of Electrical and Mechanical Engineering (NUST). Secondly, in recent years, several sensors based on split rings have been proposed for characterization and sensing of material properties using non-invasive / non-destructive methods. Thirdly, split ring based resonant structures form the basis of unit cell used for realization of meta-materials exhibiting negative permeability. Split ring based structures provide an opening for future research in the field of meta-materials.

Figure 1.1 Typical split ring with one slot

1.2 Problem Description and Objectives

Objective of this research is to find a suitable dimensional configuration of split ring resonators (SSRs) to achieve considerable shift in resonant frequency so that this structure can be tuned over a relatively broad range. Second objective is formulation of analytical solution for optimized design for approximation of resonant frequency based on simulated results in ANSYS HFSS®.

1.3 Challenges

Single SRRs are being widely researched for material characterization and sensing applications. Whereas structures based on dual split rings are being researched for application in meta-material exhibiting negative permittivity and permeability. Very small shift in resonant frequency in the range of few tens of MHz has been reported. This shift in resonant frequency is not enough to tune the structure to multiple frequencies. Objective of research poses various challenges to research configurations based on single and dual split rings enclosed within a metallic shield.

1.4 Structure of thesis

This thesis has been divided into six main chapters. Chapter 1 provides a brief introduction about the problem area and objective of research. Chapter 2 presents literature review regarding proposed applications of split ring based designs, analytical models for approximation of resonant frequency and quality factor of split ring based resonators followed by their use for material characterization and meta-materials. Chapter 3 explains the proposed methodology. Chapter 4 describes the simulation of proposed configurations in ANSYS HFSS® and their analysis followed by an optimization of selected configuration. Chapter 5 is related to development of analytical model in line with the simulated data. This chapter also compares the analytical results with simulated data. Finally, Chapter 6 concludes the thesis and mentions future work. The outcomes of this study proved to be highly satisfying and successful. Outcome of this study was published in M. Shoaib [1].

CHAPTER 2

LITERATURE REVIEW

LITERATURE REVIEW

Structures similar to split rings have been reported for design of magnetron amplifiers as early as 1940s by G. B. Collins [2], dispersion ESR Hyde [3] and acceleration of charged particles Delayen [4]. The major work in the domain of split rings started in 1980s when a number of techniques and models were presented to estimate the key parameters of these structures such as resonant frequency and quality factor.

Resonant frequency of rectangular or cylindrical cavity resonators can be tuned easily by modification of shape of the cavity or introducing some dielectric of materials. *Perturbation method* assumes that the actual fields of a cavity with a small shape or material perturbation are not greatly different from those of the unperturbed cavity, D. Pozar [5]. The detailed techniques for perturbation based method along with related theory have been provided by L. F. Chen [6].

2.1 Basic Split Ring Configuration

Basic split ring resonator consist of a cylindrical ring with slot(s) as shown in Figure 2.1. The structure shown in the figure can be considered as capacitor and single turn inductor T. Ejaz [7]. Figure 2.1 shown important physical dimensions of structure which will be used in this report. Split ring is enclosed in a cavity (termed as shield in this literature) to avoid power losses due to radiation at high frequencies. Relative

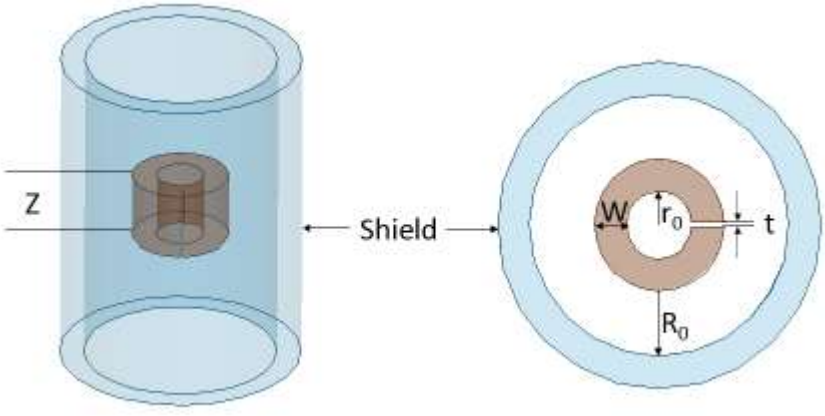

Figure 2.1 Basic split ring resonator configuration and its cross-sectional view [7]

dimensions of shield effect resonant frequency of the resonant structure. Shield is generally made of a conductive metal or some other material with conductive coating on it.

2.2 Literature Review

Miniature lumped element circuits for microwave application in X band were described as early as 1976 by D. Daly [8] in form of interdigital capacitor and loop inductor. These lumped elements were etched on an MIC substrate. Various configurations of split ring or loop gap based resonant structures have been described in literature. These configurations have been designed to meet specific application and analytical formulations have been proposed to estimate resonant frequency and quality factor. This section lists down references to some important literature related to theory, development and application of split ring based resonant structures. D. Pozar [5] provides basic concepts and theory related to cavity resonators of rectangular and cylindrical configurations. This book also briefly discusses perturbation methods to tune cavity resonators using perturbation methods. L.F. Chen [6] provides detailed theory and techniques for use of perturbation based techniques to characterize materials and calculate the dielectric constant. Spit ring based techniques have been discussed to characterize materials.

W. Hardy [9] describes a split ring resonator design for use in 200 – 2000 MHz range to achieve magnetic resonance with high quality facto. Conventional cavities become unsuitable due to their large size at these frequencies. Approximate theory for approximation of resonant frequency and quality factor has also been developed based on the energies stored in the electric and magnetic fields. This design incorporates the effect of shield on resonant frequency and quality factor. The analytical formulations have been summarized by T. Ejaz [7] which are as under for resonant frequency and quality factor:

$$f_o = \frac{c}{2\pi r_o}\sqrt{\frac{t}{\pi W}}\sqrt{1+\frac{r_o^2}{R_o^2-(r_o+W)^2}} \qquad (2.1)$$

$$Q = \frac{r_o}{\delta} \frac{1 + \frac{r_o^2}{R_o^2 - (r_o + W)^2}}{1 + \left(1 + \frac{W}{r_o} + \frac{R_o}{r_o}\right)\left(\frac{r_o^2}{R_o^2 - (r_o + W)^2}\right)^2} \tag{2.2}$$

Where f_o represents resonant frequency, Q represents the quality factor, c is speed of electromagnetic radiation in free space, μ_o is permeability of free space and δ is the skin depth of resonator material.

W. Froncisz [10] studied SRR with multiple gaps and developed equations to approximate resonant frequency for its use in ESR spectroscopy between 1 to 10 GHz. Gap capacitance and loop inductance has been calculated to estimate the resonant frequency. No of gaps can be increased and capacitances of theses individual gap can be connected in series. T. Ejaz [7] modified the design equation to be used for a ring with single gap. This design also incorporates effect of shield in design equations. These equations are given as under:

$$f_o = \frac{c}{2\pi r_o}\sqrt{\frac{t}{\pi W}} \tag{2.3}$$

$$f_o = \frac{c}{2\pi r_o}\sqrt{\frac{t}{\pi W}}\sqrt{1 + \frac{r_o^2}{R_o^2 - (r_o + W)^2}}\sqrt{\frac{1}{1 + \frac{2.5t}{W}}} \tag{2.4}$$

Equation (2.3) does not include effect of shield whereas Equation (2.4) includes effect of shield in the design for approximation of resonant frequency. Internal radius of shield should be less than the cut off wavelength for the lowest excited propagation mode in a cylindrical waveguide without split rings.

M. Mehdizadeh [11] proposed split rings for 1-4 GHz frequency range. Various methods for tuning of resonant structure to a desired frequency and coupling methods have been discussed. Axial and radial dimensions of shield should be large enough to accommodate the magnetic field lines around the split ring.

M. Mehdizadeh [12] published their design equations in 1983 and 1989. These equations also include the effect of fringing electric and magnetic field on resonant

frequency in addition to the effect of shield. Design equations ate given as under:

$$f_o = \frac{c}{2\pi r_o}\sqrt{\frac{t}{\pi W}}\sqrt{1+\frac{r_o^2}{R_o^2-(r_o+W)^2}}\sqrt{\frac{1+\frac{\Delta Z}{Z}}{1+\frac{\Delta W}{W}}} \tag{2.5}$$

$$\Delta Z = 0.18R_o\,, \Delta W = 3t \tag{2.6}$$

Where Z is the length of the resonator (as per Figure 2.1), ΔZ and ΔW are length extension due to fringe effect of magnetic field and electric field respectively. Uniform magnetic fields and electric fields have been assumed in the length extensions defined by ΔZ and ΔW. The expressions to approximate ΔZ and ΔW have been shown in Equation (2.6); found by curve fitting of experimental data.

Jia-Sheng Hong [13] presents theory and experiments of microwave filters based on split ring resonators. The most attractive feature if these filters in their micro-strip based fabrication and compact size.

J. Pendry [14] showed that microstructures built from nonmagnetic conducting sheets exhibit an effective magnetic permeability, which can be tuned to values not occurring naturally. Many magnetic permeabilities can be achieved using variation of different parameters of split rings.

C. Enkrich [15] discussed use of split ring based microstructures and meta-materials for telecommunication and visible spectrum in terahertz range.

S. Eaton [16] presented another set of design equations based on earlier works of W. Froncisz [10] and M. Mehdizadeh [11]. This solution considers coupling conditions whereas effect of shield has been ignored. Expression for resonant frequency is given as:

$$f_o = \frac{1}{2\pi\sqrt{LC}} \tag{2.7}$$

Where inductance and capacitances are given as

$$L = \frac{\mu o \pi r_o^2}{Z + 0.9r_o} \tag{2.8}$$

$$C = \varepsilon_r \varepsilon_o \frac{(W+t)(Z+t)}{t} \tag{2.9}$$

A. Masood [17] presented a split ring resonator based technique for compositional analysis of solvents in microcapillary systems in 2008. This technique showed that split ring based sensors can be developed for analysis of materials.

O. Sydoruk [18] proposed presence of two different types of capacitances in the structure of split ring; gap capacitance and surface capacitance. Analytical expressions for calculation of surface and gap capacitance of split ring resonator have been developed. It has been also established that at very small gaps/splits, gap capacitance dominates whereas surface capacitance becomes a major contributor as gap increases. The resonant frequency can be calculated from Equation (2.7). Inductance of the split ring has been approximated in Equation (2.10) using formulae for one turn inductor given in F. W. Grover [19]. The derived expressions for gap and surface capacitance are given by Equations (2.11) and (2.12):

$$L = \frac{\mu o \pi r_o^2}{Z + 0.9 r_o} \tag{2.10}$$

$$C_{gap} = \varepsilon_o \left(\frac{ZW}{t} + Z + W + t \right) \tag{2.11}$$

$$C_{surface} = \frac{2\varepsilon_o (Z+W)}{\pi} log \frac{4r_o}{t} \tag{2.12}$$

The total capacitance is sum of gap and surface capacitance which is given as:

$$C_{total} = C_{gap} + C_{surface} \tag{2.13}$$

F. Capolino [20] describes use of various split ring based structures for realization of meta-materials. Approximate expressions for calculation of resonant frequency are also discussed base on J. Pendry [14]. Broadside coupled configuration will show more shift in resonant frequency as compared to complementary split rings configurations. The capacitance of split rings can be added in parallel and average values of self-inductance of split rings is taken for calculation of resonant frequency of complementary split rings. These assumptions can be held firm for broad side couple split rings.

C. Balanis [21] provides a comprehensive survey regarding evolution and development of mate-materials and use of split ring based structures to achieve double negative characteristics. This book also provides detailed theoretical background for cavity resonators. Cylindrical configuration of shield (which can also be considered as a cylindrical cavity) offer higher quality factor as compared to rectangular shields. This can be attributed to reason that circular cavity does not possess as many sharp corners and edges. The volume and surface area of rectangular cavity are not well utilized by the interior fields.

A. Abduljabar [22] proposed a new type of microwave microfluidic sensor based on split ring to detect and determine the dielectric properties of common polar liquids. The technique is based on perturbation theory, in which the resonant frequency and quality factor of the microwave resonator depend on the dielectric properties of the resonator. Electric field within split of ring is perturbed by presence of liquid in a capillary tube. Sensor design uses micro strip based planer split ring with two gaps at 3 GHz.

D. Rowe [23] presents a method to achieve a low loss split ring resonator for microfluidic sensing of polar liquids at microwave frequencies. In this method, split ring made of silver coated copper wire with square cross section and inward extended legs has been demonstrated to show improved results than conventional split rings. This geometric manipulation of design enhanced confinement of electric field in the capacitive region of split ring. Resonant frequency is predominantly set by ring radius and both are inversely proportional, and partly set by the capacitive gap. Approximate expressions developed by curve fitting of simulated data are as under:

$$f_o = 0.0168r^2 - 0.502r + 5.19 \tag{2.14}$$

$$Q = -8.8r^2 + 78r + 1810 \tag{2.15}$$

where f_o is resonant frequency, Q is quality factor and r is the radius of silver coated copper split ring placed inside a metallic shield. Optimized parameters of split ring and shield have been used from T. Ejaz [7] and A. Abduljabar [22], for design of dimensional configurations. The dimensional configuration used for development of 3-D

model in ANSYS HFSS® and simulation are given in Table 3.3. Effect of change in various parameters such as inner radius, split, height of wire, width of wire have been modeled and simulated.

TABLE – 3.3: OPTIMIZED DESIGN PARAMETERS FOR SINGLE SRR SIMULATION

Parameter	Design value
Inner radius of cavity	19 mm
Shield thickness	7 mm
Height of shield	30 mm
Inner radius of split ring	10 mm
Capacitive gap (split) or ring	1.5 mm
Height of ring wire	1 mm
Width of ring wire	1 mm
Geometry of ring wire	Square
Material of shield	Aluminum
Material of rings	Copper
Space inside cavity	Air

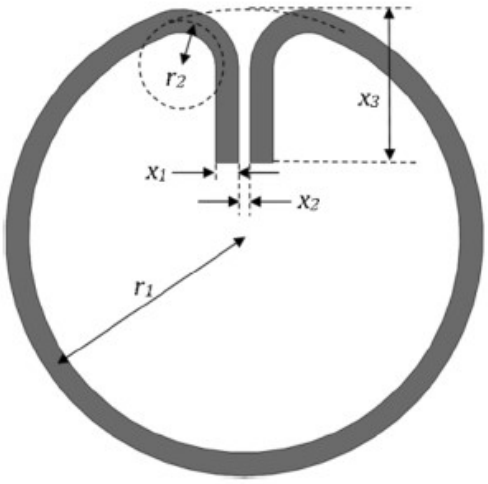

Figure 2.2 – Design of split ring configuration used for microfluidic sensing [23]

T. Ejaz [7] presents a comparative analysis of analytical models developed by W. Hardy [9], W. Froncisz [10], M. Mehdizadeh [12], S. Eaton [16] and O. Sydoruk [18]. Two key parameters have been calculated and compared with simulated results from ANSYS HFSS® [24]. An analysis is presented for the correctness and validity of models for various dimensional configurations of split rings. Analysis revealed that none of the models could accurately yield the simulated results. It is very important to incorporate all the parameters including effect of shield, effect of fringing fields, and material of structure to get the results closer to simulated values. Every dimensional configuration requires its own set of equations to approximate resonant frequency and quality factor.

A noninvasive and continuous blood glucose monitoring sensor topology based on dual split rings has been proposed by H. Choi [25] and validated with *in vivo* and *in vitro* interference

tests. One split ring is used as a reference and other is used for sensing. Rings are placed in broad side coupled configuration and have slightly different dimensions.

M. Wellenzohn [26] proposes a theoretical design of a biosensor device based on split ring resonators for operation in the microwave regime.

Xutao Tang [27] has demonstrated a method to control the resonant frequency of micro-strip based broadside coupled split ring resonators using pneumatic pressure. Air pressure serves to regulate the vertical levitation between the two discs of dielectric material containing micro-strip split rings etched on a board. Measured and simulated results have been shown to agree.

T. Hayat [28] presents a simulation based comparative analysis of split rings for compositional analysis of polar solvents using micro capillary arrangement. Electric field perturbation has been used to sense the change in permittivity of medium in the capacitive split of the ring.

T. Ejaz [29] presents a technique to develop shield around a split-ring resonator to give optimized quality factor. Regression equations have also been developed based on this technique and statistical analysis for estimation of resonant frequency and quality factor. Different materials have been considered for fabrication of shield and it has been

established with simulated and experimental data that Aluminum provides optimum results when used for fabrication of shield.

R. Alahnomi [30] proposed a symmetrical split ring resonator (SSRR) based design for performance enhancement of microwave sensors. Design can be used for various industrial applications such as food industry, quality control, bio-sensing, medicine and pharmacy. This paper has illustrated its use for sensing and characterization of meat samples.

CHAPTER 3

METHODOLOGY & SIMULATION

METHODOLOGY AND SIMULATION

Dimensional configurations of split ring resonator include dimensions of split ring and shield. A typical split ring resonator along with the outer shield is shown in Figure 3.1. Split rings and shield of cylindrical geometries have been considered in this research only. Variation in following dimensions of single split ring resonator (enclosed in a shield) can result in shift in resonant frequency:

- Radius of split ring
- Gap / split of ring
- Width of ring
- Height of ring

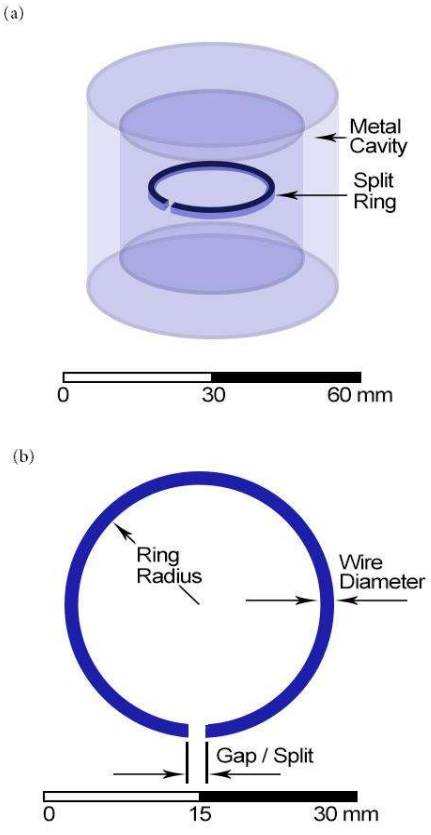

Figure 3.1 - Design structure for a) split rings within metallic cylindrical shield (b) split ring showing the gap/ split

- Material of ring
- Inner radius of shied
- Height of shield

This configuration consists of single split rings resonator. The single ring inside shield can be replaced with the dual split ring for dual split ring base configuration. At first, dimensional configurations of single split ring based resonator have been worked out for simulation in ANSYS HFSS®.

Dimensional configurations of split rings have been grouped as under:

- Split ring resonator with single ring
- Dual split ring resonator – Complementary split rings

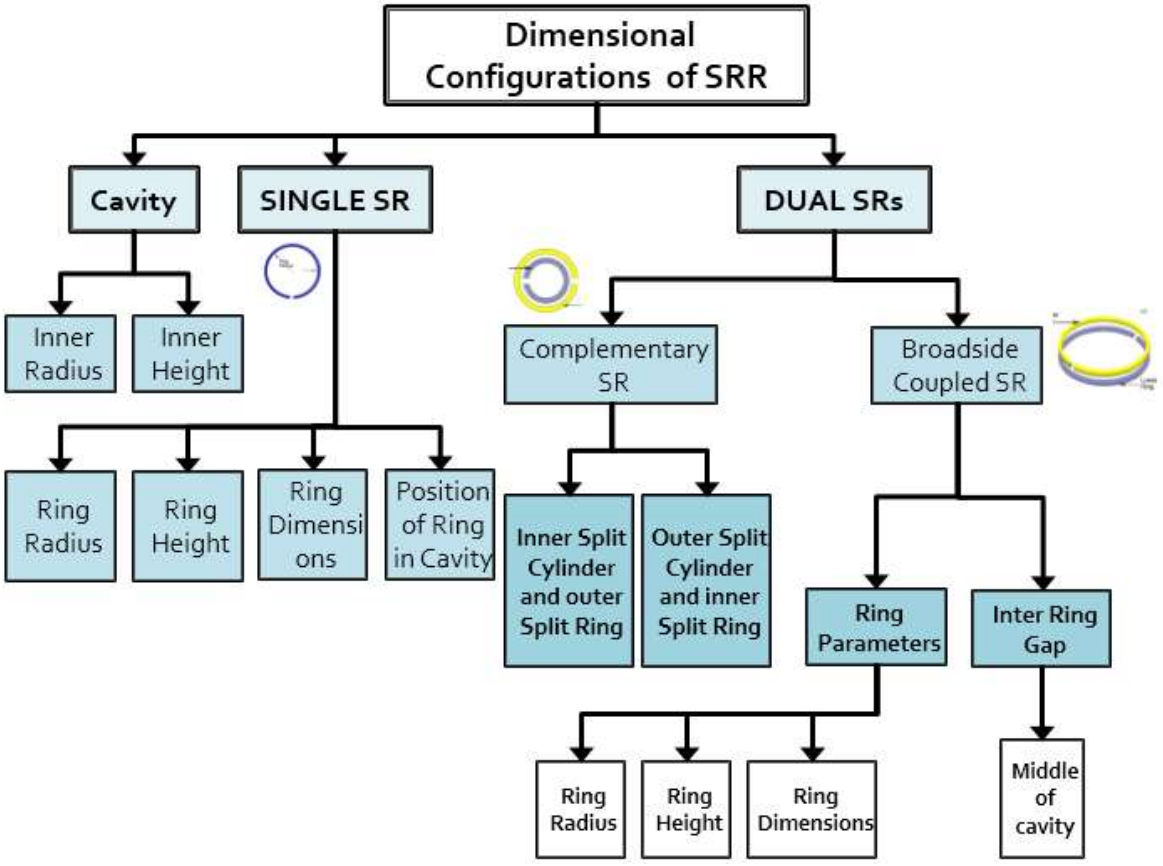

Figure 3.2 – Flow chart of research methodology to find a suitable configuration for shift in resonant frequency

- Dual split ring resonator - Broadside coupled split rings

Methodology to find a suitable configuration to achieve desired shift in resonant frequency is shown in Figure 3.2 in form of a flowchart.

3.1 Single Split Ring Resonator

Single split ring resonator is simple configuration which has extensively been researched for material characterizations. Material characterization makes use of intensity of electric field with the capacitive gap of the ring. Sample under test is placed within the gap and perturbation caused is measured in terms of shift in resonant frequency and quality factor. In this method, very small shift in resonant frequency is achieved which is not sufficient for tunability of resonator. Dimensional configurations of single split ring based design are discussed in following sub-sections which can result in considerable shift in resonant frequency.

3.1.1 Verification of Already Published Design for Single Split Ring

D.J. Rowe [23] is one of the recent published works which utilized single split ring of square wire cross section to carry out microfluidic sensing. The dimensional configurations of this design are given in Table 3.1. Legs of the split rings have been extended inward to enhance the intensity of electric field by increasing the capacitive area of gap. Various dimensional parameters and material selection for this configuration is shown in Figure 3.3.

TABLE 3.1 - PARAMETERS OF SPLIT RING USED FOR MATERIAL CHARACTERIZATION [23]

Parameter	**Unit**	**Value**
Ring radius (r_1)	mm	12.5
Wire profile / cross section		Square
Thickness (x_1)	mm	1
Leg separation (x_2)	mm	1.5

Parameter	Unit	Value
Leg length (x_3)	mm	6
Shield radius	mm	19
Shield height	mm	30
Material of ring	Silver coated copper wire	
Material of shield	Aluminum plated with silver	

This configuration was simulated by the authors with COMSOL®. The same configuration has been simulated in ANSYS HFSS®. Table 3.2 shows the comparison between published and simulated results with ANSYS HFSS®.

TABLE 3.2 – COMPARISON BETWEEN PUBLISHED [23] AND SIMULATED RESULTS

Parameter	Published result simulated with COMSOL [23]	Simulated with Ansys HFSS
Resonant Frequency (GHz)	1.52	1.37
Quality Factor	1200	1120

It can be seen that results are similar. The variation can be attributed to different software configurations and techniques to compute the resonant frequency and quality factor. After the verification of own effort with published results, various configurations have been simulated in ANSYS HFSS® to observe shift in resonant frequency.

3.1.2 Various Dimensional Configurations

Include in Literature survey

3.1.2.1 Vertical Position of Split Ring inside Shield

Position of split ring was changed along the axis of the shield. Initially split ring was placed 1 mm above the bottom of shield and gradually moved upward till its gap from top of the shield is 1 mm. Simulated results obtained from ANSYS HFSS® by parametric analysis are shown graphically in Figure 3.4a. No significant shift in resonant frequency is observed with change of vertical position of split ring within metallic shield.

3.1.2.2 Inner Radius of Split Ring

Inner radius of split ring was varied from 6 to 15 mm while keeping other parameters fixed as noted in Table 3.3. Simulated results obtained from HFSS by parametric analysis are shown graphically in Figure 3.4b. Resonant frequency decreased as radius if split ring increased.

3.1.2.3 Split of Split Ring

Split (capacitive gap) of ring was varied from 0.5 mm to 3 mm while keeping other parameters fixed as noted in Table 3.3. Simulated results obtained from HFSS by parametric analysis are shown graphically in Figure 3.4c. Shift in resonant frequency was observed for small split (gap). Shift became insignificant with large gaps.

3.1.2.4 Height and Width of Split Ring

Height of split ring was increased from 1mm to 10mm while split ring place at middle of the cavity. Other parameters were kept fixed as in Table 3.3. Similar width of split ring was varied from 1mm to 5 mm. Simulated results did not show significant shift in resonant frequency.

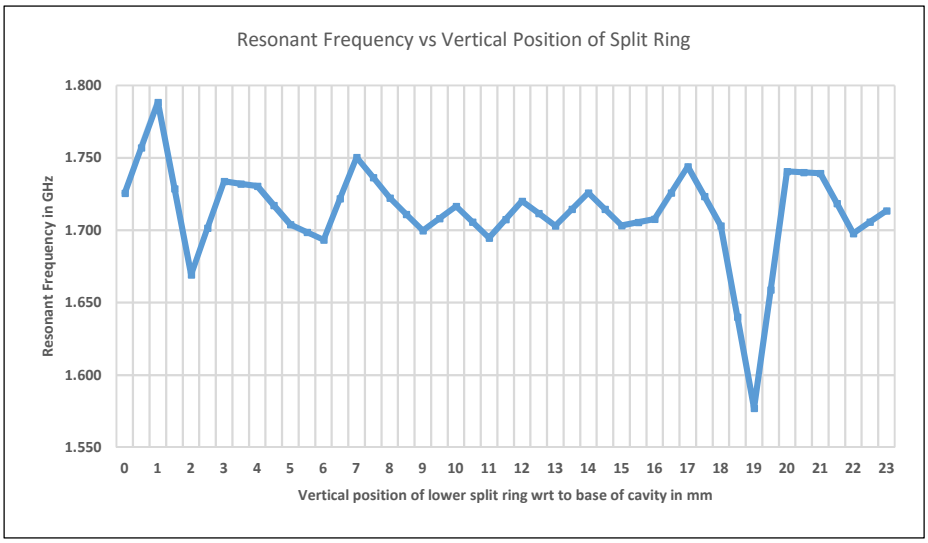

Figure 3.4 a - Resonant frequency of single SSR with variation of vertical position of SR along cavity axis

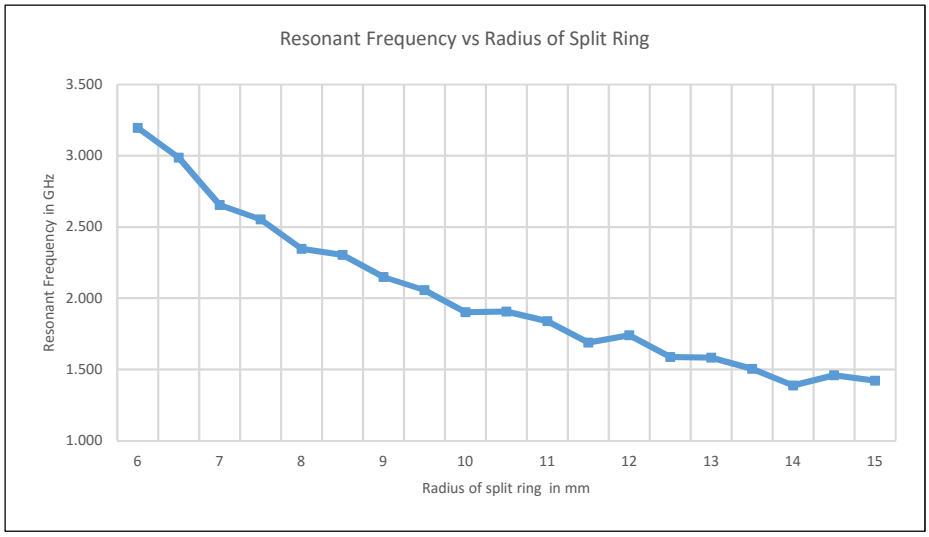

Figure 3.4 b – Shift in resonant Frequency with variation in radius of split ring

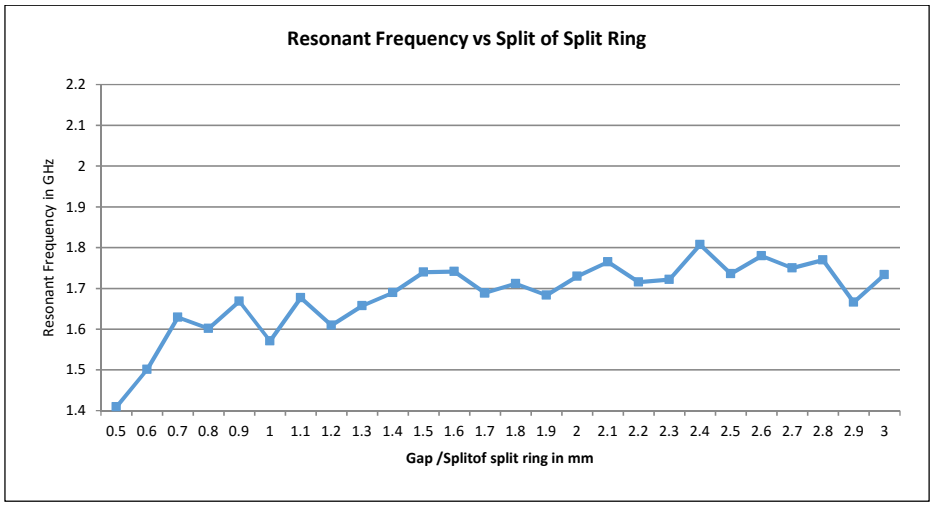

Figure 3.4c – Shift in resonant Frequency with variation in capacitive gap / split of SR

3.2 Dual Split Ring Resonator – Complementary Split Rings

Complementary spit rings are one of the dual configurations which consists to two co-planer split rings of different radii. Ring with smaller radius is placed inside the ring with larger radius. The splits of both the rings are generally placed 180^{o} apart to ensure maximum coupling. This configuration is widely used to achieve negative permeability in meta-materials [21]. This configuration of split rings is illustrated in Figure 3.5.

Various positions of split rings within the shield have been simulated and shift in resonant frequency observed. Configurations very near to bottom and top of shield have not been considered as these will not ensure uniform distribution of magnetic field lines inside shield. Positions in the middle of the shield are likely to provide maximum uniformity to magnetic and electric fields. It can be observed from Figure 3.4b that smaller radii provide relatively larger shift in resonant frequency than the larger one. The radii of complementary split rings are selected to be between 6-9 mm as this range of radii has shown maximum shift in resonant frequency during simulation single split ring configuration. Selected parameters for complementary split rings are listed in Table 3.4.

TABLE – 3.4: DESIGN PARAMETERS FOR DUAL COMPLEMENTARY SPLIT RING CONFIGURATION

Parameter	Design value
Radius of outer SR	8 mm
Radius of outer SR	6 mm
Capacitive gap (split) or ring	1.5 mm
Dimension of ring wire	1mmx1mm
Geometry of ring wire	Square
Material of cavity	Aluminum
Material of rings	Copper
Space inside cavity	Air

Four dimensional variations were simulated for this configuration of split rings.

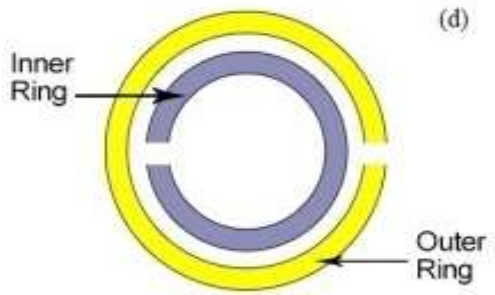

Figure 3.5 – Typical layout of dual complementary split ring configuration

These configurations are listed briefly in following sub-sections.

3.2.1 Option-I

Inner SR is placed 10 mm above base of shield and remains stationery for this configuration Outer ring is gradually moved upward along axis of the shield form 10 mm to 20 mm. The dimensions and geometry of ring wires are same for the inner and outer split rings. 3-D model is developed and simulated in ANSYS HFSS®. Shift in resonant frequency has been plotted in Figure 3.6a.

3.2.2 Option-II

In this dimensional configuration, outer split ring is placed fixed at 10 mm above base of shield and inner split ring is gradually moved upward along axis of the shield form 10 mm to 20 mm. The dimensions and geometry of ring wires are same for the inner and outer split rings. 3-D model is developed and simulated in Ansys HFSS. Shift in resonant frequency has been plotted in Figure 3.6b.

3.2.3 Option-III

In previous two configurations, height and width of both the split rings was similar. In third and fourth option, the heights of inner and outer rings have been varied. In this configuration height of inner split ring is changed to 10 mm forming a split cylinder. Split cylinder is placed 10 mm above base of shield and kept fixed. Outer split ring dimensions are maintained as per Table 3.4 and gradually moved upward along axis of shield. The simulated shift in resonant frequency is plotted in Figure 3.6c.

3.2.4 Option-IV

In this configuration height of outer split ring is changed to 10 mm. Both the rings are placed 10 mm above base of shield as initial position. Dimensions of inner split ring are kept as per Table 3.4 and inner split ring is gradually moved up along axis of cavity. The shift in resonant frequency is plotted in Figure 3.6d.

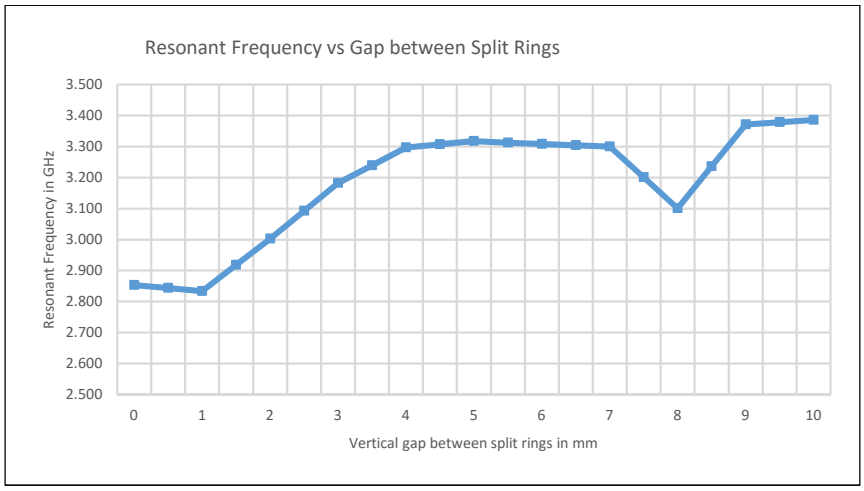

Figure 3.6a – Shift in resonant frequency – Option-I

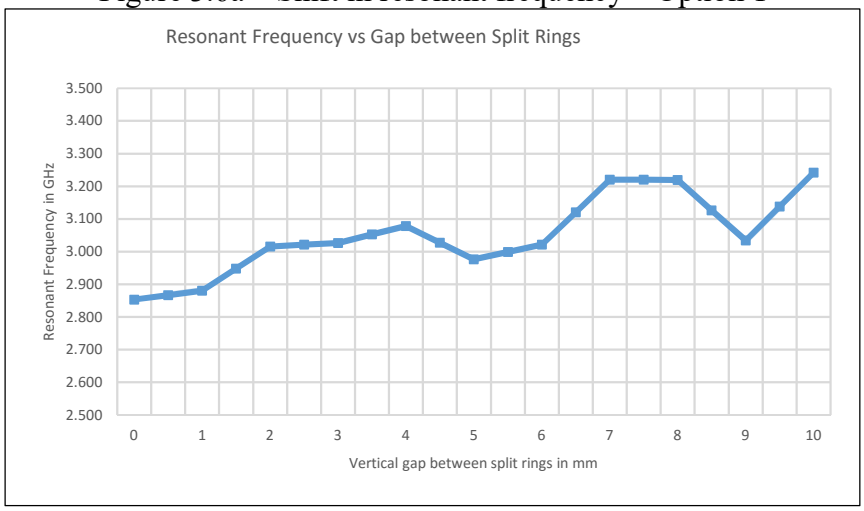

Figure 3.6b – Shift in resonant frequency – Option-II

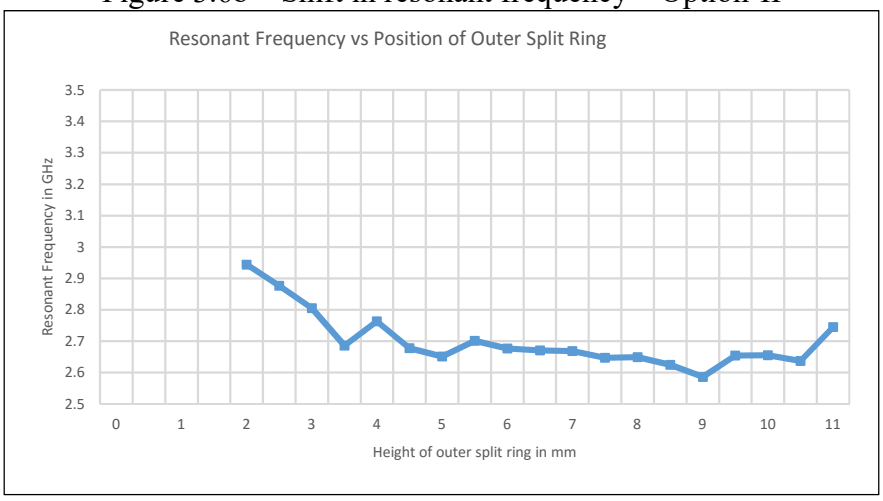

Figure 3.6c – Shift in resonant frequency – Option-III

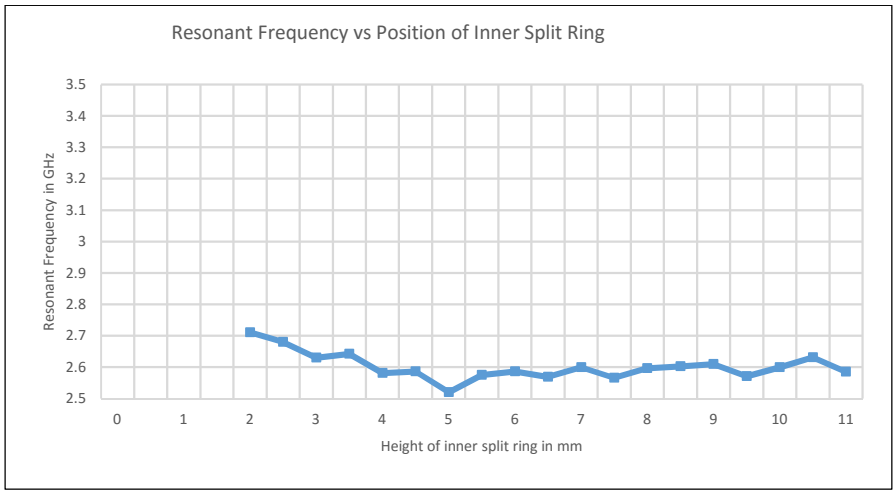

Figure 3.6d – Shift in resonant frequency – Option-IV

3.3 Dual Split Ring Resonator – Broadside Coupled Split Rings

In this configuration, two rings of similar radii, cross section and material are vertically stacked along axis of the shield with gap between them. The splits of these rings are positioned 180° apart to ensure maximum coupling as in case of complementary split rings. This type of configuration can provide greater shift in resonant frequency owing to increased capacitance between the rings [20]. In these configurations one ring is kept static (fixed) at a position within the shield and other is moved relative to fixed ring over 10 mm. [27] has demonstrated shift in resonant frequency of micro-strip based broadside couple resonators when one ring is moved 0.2 mm away from stationary ring. Typical configuration is shown in Figure 3.7 for two broadside coupled split rings. Design parameters for this configuration are listed in Table 3.5.

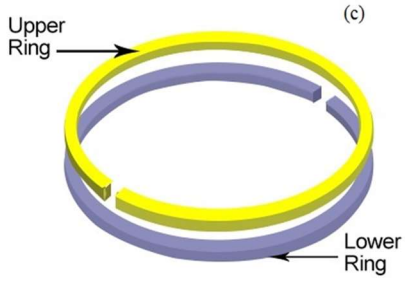

Figure 3.7 – Typical layout of dual complementary split ring configuration

TABLE – 3.5: DESIGN PARAMETERS FOR DUAL BROADSIDE COUPLED SPLIT RING RESONATOR

Parameter	Design value
Radius of inner and outer split rings	10 mm
Capacitive gap (split) or ring	1.5 mm
Dimension of ring wire	1mmx1mm
Geometry of ring wire	Square
Material of shield	Aluminum
Space inside shield	Air

Two options were simulated for this configuration. Options with split ring placed near bottom and top face of shield are not considered due to reasons mentioned earlier.

3.3.1 Option-I

Lower ring was placed fixed 1 mm above the bottom of the shield. Upper split ring was place 1 mm above the fixed lower split ring. Upper split ring was moved gradually over a distance of 10 mm from its initial position. Simulated shift in resonant frequency was recorded through parametric analysis in ANSYS HFSS®. Simulated shift in resonant frequency is plotted in Figure 3.8a.

3.3.2 Option-II

This option is similar to option I with the difference that lower split ring is placed 10 mm above base of cavity. Simulated shift in resonant frequency is plotted in Figure 3.8b.

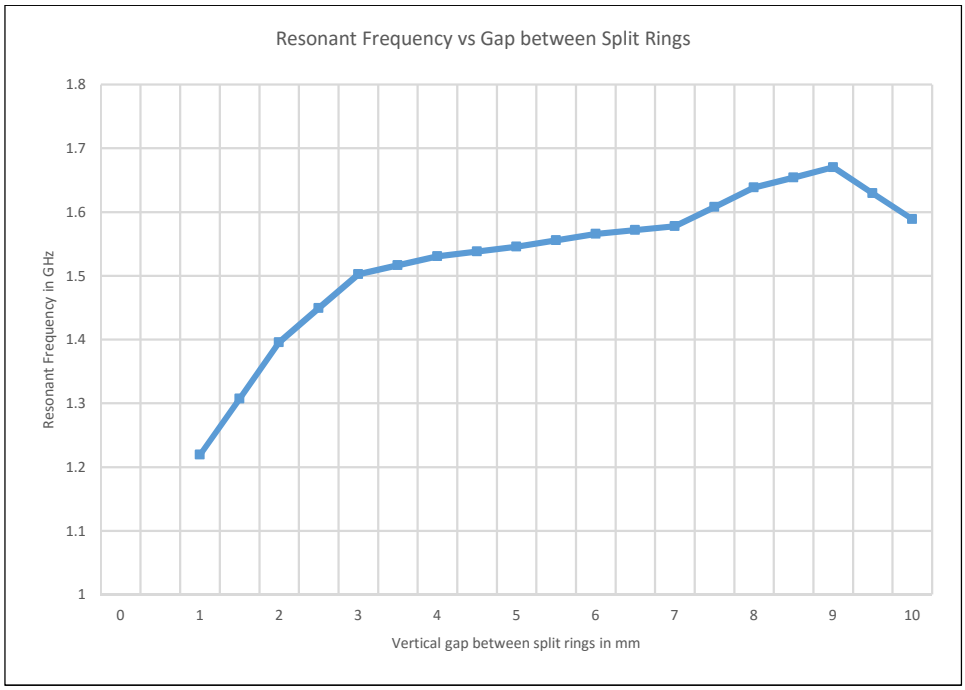

Figure 3.8a – Shift in resonant frequency – Option-I

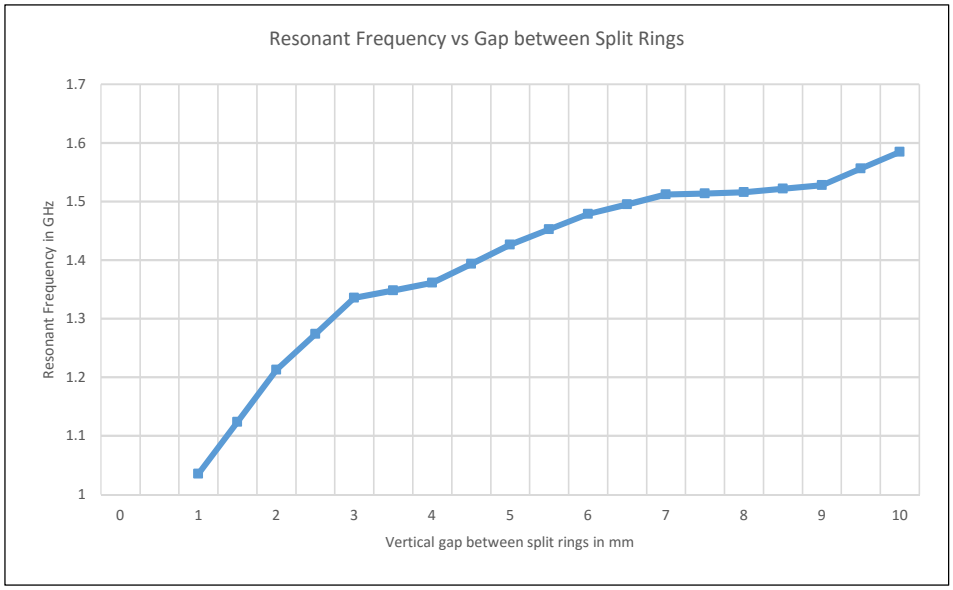

Figure 3.8b – Shift in resonant frequency – Option-II

3.4 Analysis of Simulated Configurations

Data of results of three configurations of split ring resonators have been analyzed and discussed with a focus on amount of shift in resonant frequency in following section.

3.4.1 Single Split Ring Resonator

From the results of simulations in ANSYS HFSS®, it can be observed that tunability over a considerable broad range cannot be achieved by change of position of split ring along axis of the shield. This can be attributed to the fact that inner surface areas of shield and split ring remained unchanged in this configuration which resulted in stable resonant frequency. Some irregularities are observed for positions of ring very near to shield's base and top. These can be due to interaction of fields of split ring with the shield surface. This aspect is not covered in this research as uniform distribution of electric and magnetic fields has been assumed [11].

A significant shift in resonant frequency was observed when radius of split ring was varied from 6 to 15 mm. Change in radius changed surface area of split ring however split (capacitive gap) was maintained for all radii. Change in radius changed overall self-inductance and surface capacitance of split ring [18]. Resonant frequency decreased with increase in ring radius showing inverse proportion. This option provides maximum shift in resonant frequency for tunability of resonator. This option is limited by difficulties to implement variable radius of a metallic ring inside cavity. However, this analysis provides an insight to the range of radii of SR which provide maximum shift in resonant frequency.

Shift in resonant frequency is also observed for change in split. Resonant frequency becomes stables for larger splits. In this case shift in resonant frequency is due to change in capacitance caused by the split between the split faces. Self-inductance and surface capacitance remains largely unchanged. However, gap capacitance increases sufficiently as split reduces. Overall capacitance of SR is combination of surface capacitance and gap capacitance. Gap capacitance dominates at narrow gaps only causing resonant frequency to shift.

Change in height and width of split rings does not provide signification shift in resonant frequency required for tunability of resonator. Furthermore, these options are not practically easy to implement for metallic split rings.

3.4.2 Dual Split Ring Resonator – Complementary Split Rings

Shift in resonant frequency has been observed for various options of complementary split ring configurations. This configuration can also be considered for tunability of split rings as it provides significant shift in resonant frequency. Detailed observation of simulated data reveals large variations in adjacent values. This configuration can be easily implemented and a mechanism to move / displace complementary split rings can be designed.

3.4.3 Dual Split Ring Resonator – Broadside Coupled Split Rings

In case of broadside coupled configuration of split rings, considerable shift in resonant frequency is achieved in both the simulated configurations. This shift in resonant frequency can be attributed to change in the broad side coupling of two dual split rings as inter ring gap is varied. Increase in gap between the rings reduces the broad side coupling and hence results in shift in resonant frequency. Although split rings placed near the bottom of the shield provide better shift in resonant frequency however this configuration is not considered viable as it violates the basic assumptions for the uniformity of the fields.

This configuration can also be implemented practically with development of a mechanism for precise and smooth movement of one of the dual rings along axis of the shield.

3.4.4 Comparison between Single and Dual Split Ring Configurations

Results of ANSYS HFSS® simulations for single, dual complementary and broadside coupled split rings have been plotted in a combined form in Figure 3.9 for purpose of comparisons. Horizontal axis in plotted figure represents vertical position of split ring and radius of radius of split ring in mm for single split ring configuration, inter ring gap in mm for dual configurations of complementary and broadside coupled split rings.

Broadside coupled configuration of split rings is the most suitable to achieve considerable shift in resonant frequency due to the reasons listed below:

- Broadside coupled configurations provide 0.55 GHz and 0.45 GHz shift in resonant frequency over 10 mm of inter ring gap, more than that of single split rings (less change in ring radius) and complementary split rings.
- Shift in resonant frequency is smoother as compared to complementary configuration.
- It is easy to model smooth shift in the resonant frequency (smooth curve) by analytical modeling and curve fitting techniques.

It is pertinent to notice that for large vertical gap between the split rings for broadside coupled configuration (See broadside inset in Figure 3.9), the values of resonant frequency approach the values for single split ring configuration. This shows that the coupling between the two rings at these values of inter ring gap has weakened to the minimum. Furthermore, amount of shift in resonant frequency reduces with increase in inter ring gap. This phenomenon indicates dependence of resonant frequency on inter

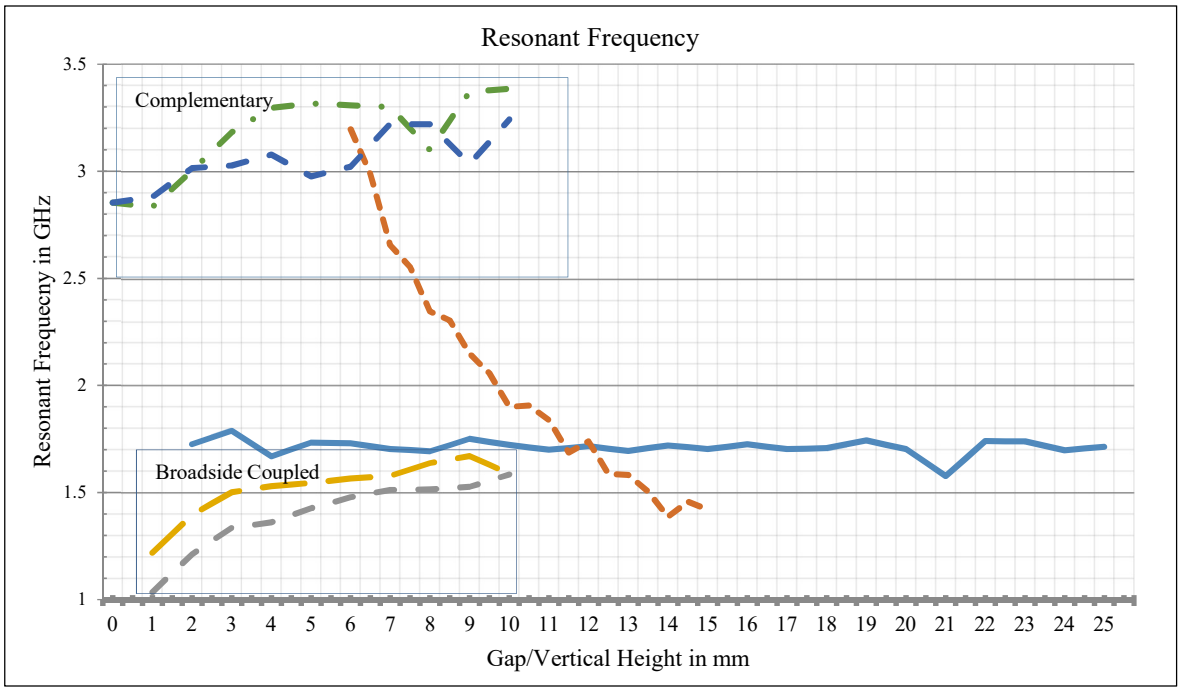

. Figure 3.9– Comparison of various configurations for shift in resonant frequency

ring gap.

Complementary split ring configuration also provide considerable shift in resonant frequency however this configuration has not been researched further due to following aspects:

- Simulated shift in resonant frequency is less than broadside coupled configuration.
- Shift in resonant frequency is very sharp for small inter ring gaps and minimal shift after that.
- Large number of irregularities in simulated data points as compared to broadside couple configuration.
- Relatively difficult to implement practically as compared to broadside coupled configuration.

CHAPTER 4
OPTIMIZATION

OPTIMIZATION

Broadside coupled split ring configuration was selected for optimization based on the results of simulated data of Chapter 3. The optimization has been carried out to reach dimensional configurations of dual broadside couple split ring resonators which will provide maximum shift in resonant frequency with change in inter ring gap. Quality factor of resonator has also been included as another deciding factor during this optimization. Very less variation in quality factor is required to ensure constant bandwidth and selectivity of resonator. Sharp variations in quality factor will induce big variations in bandwidth. Maximum shift in resonant frequency and minimum variance in quality factor is the optimization criteria required for dual broadside coupled split ring configuration.

This chapter covers overall optimization scheme and resultant optimized dimensional parameters of dual broadside coupled split rings configuration. Uniform electric and magnetic fields have been assumed to exit within this structure. The electric field is supported between the two parallel faces of split whereas magnetic field surround the split rings. Conduction current flows circumferentially on the inner surface of shield and split rings [12].

4.1 Optimization Scheme

Radius of split rings, shield and position of split rings inside shield has been considered for the optimization of split ring resonator. Resonant frequency and quality factor have been simulated for each dimensional variation using parametric analysis in ANSYS HFSS®.

4.2 Optimized Parameters for Shield

Split rings are enclosed inside a metallic shield to avoid losses due to radiation at high frequency. Dimensions of shied should be large enough to ensure uniformity of magnetic field inside the split ring and in the annular region between the outer surface of split rings and inner surface of shield. Various configurations of shield have been simulated in ANSYS HFSS® and following dimensions of shield have been selected:

- Inner radius of shield – 33 mm
- Inner height of shield – 30 mm
- Thickness of shield wall – 7 mm

4.3 Optimization of Split Rings

Split ring dimensions of 1mm x 1mm, square cross section have been used as these will provide maximum inter ring capacitance due to their geometry. Furthermore, capacitance in the gap will be more compared to the circular wire of 1 mm diameter. The split of 1 mm is used in both the rings. Splits are placed 180^{o} apart to ensure maximum coupling.

Second aspect for optimization of split rings is their placement inside shield along axis of shield. Available options are listed below for broadside coupled rings which have been simulated in HFSS and resultant shift in resonant frequency and variance in quality factor have been recorded.

- *Option – I*. Lower ring placed 1 mm above bottom of shield (bottom configuration)
- *Option – II*. Lower ring placed 5 mm above bottom of shield
- *Option – III*. Lower ring placed 10 mm above bottom of shield

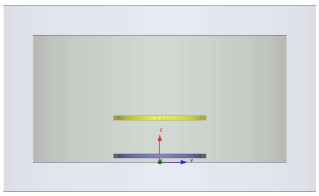

(a) Option-I (1mm)

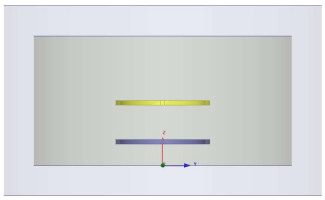

(b) Option-II (5mm)

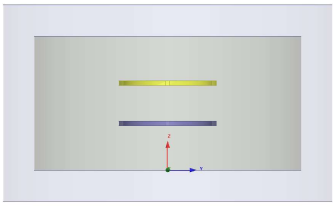

(c) Option-III (10 mm)

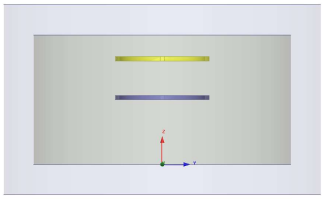

(d) Option – IV (15 mm)

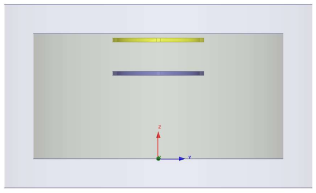

(e) Option – V (20 mm)

Figure 4.1. – Options for optimization of broadside coupled split ring configuration

- *Option – IV*. Lower ring placed 15 mm above bottom of shield (middle of shield)
- *Option – V*. Lower ring placed 20 mm above bottom of shield

For each option, upper ring is initially placed above the lower split ring with inter ring gap of 1 mm. Upper ring is moved upward gradually with a step of 0.5 mm for maximum inter ring gap of 10 mm using parametric analysis in ANSYS HFSS®. These options are shown in Figure 4.1. In addition to above, radius of split rings has also been varied from 8 mm to 12 mm using parametric analysis. Simulated results of shift in resonant frequency and quality factor will provide the values for radii of split rings which will meet the optimization criteria.

First and fifth options have not been considered in this research as enough space between the shield and rings in not available to ensure uniformity of magnetic field lines. In case of first option, lower split ring is very close to base of shield whereas in fifth option last position of upper split ring will become very close to the top surface of shield (almost 1 mm for inter ring gap of 7 mm).

4.4 Optimization with respect to Shift in Resonant Frequency

Simulated shift in resonant frequency is plotted in Figure 4.2 for various inner radii of rings for 2nd, 3rd and 4th options.

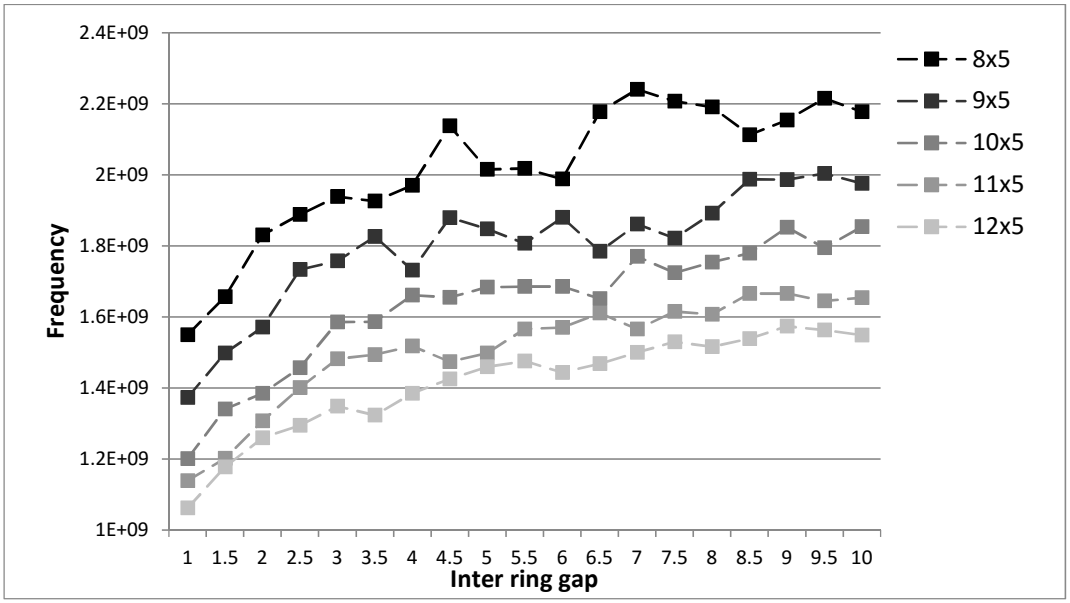

Figure 4.2a– Shift in resonant frequency for Option-II (5 mm) of dual BC-SSR for various ring radii

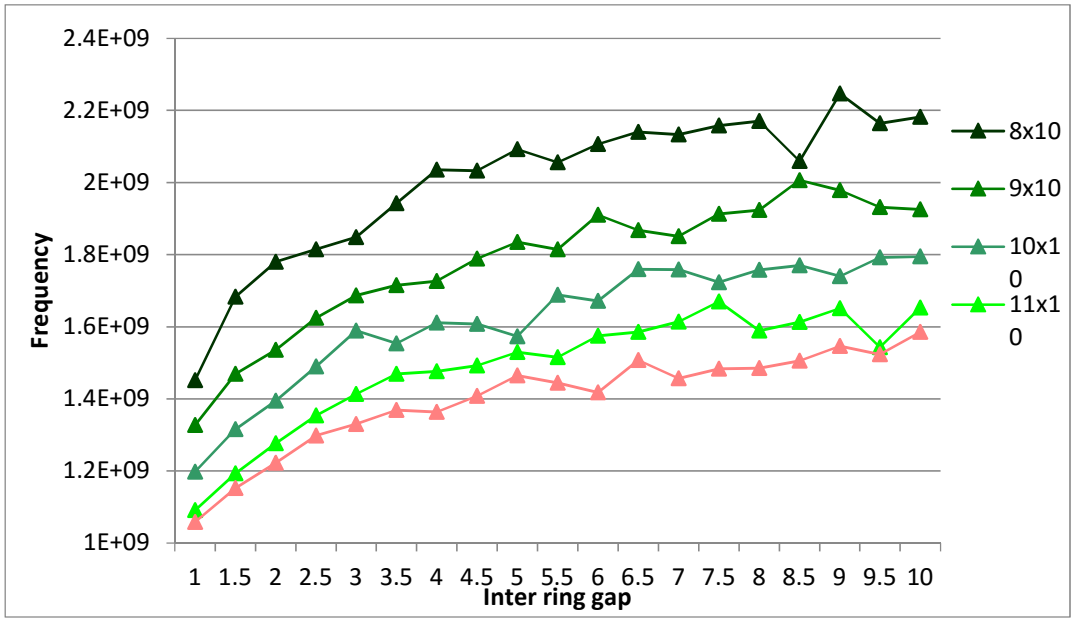

Figure 4.2b– Shift in resonant frequency for Option-III 10 mm) of dual BC-SSR for various ring radii

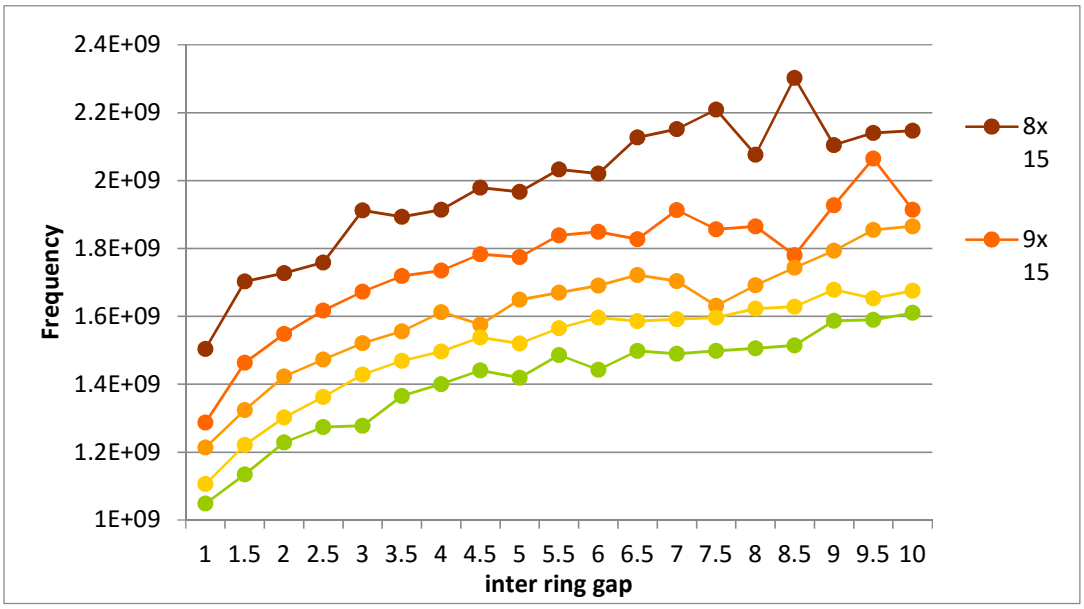

Figure 4.2c– Shift in resonant frequency for Option-IV (15 mm) of dual BC-SSR for various ring radii

Following can be inferred from detailed investigation of the plotted results in Figure 4.2 (a-c):

- Smaller radii of split rings result in higher resonant frequencies as compared to larger radii.
- Smaller radii split rings provide more shift in-between adjacent values of inter ring gap. Maximum continuous positive shift in resonant frequency is achieved within 3-4 mm of inter ring gap.
- Data points for larger radii (10, 11 and 12 mm) are regular than the smaller radii which result in smooth plot.
- Resonant frequencies for smaller radii (8, 9 mm) change abruptly for larger inter ring gaps.
- Resonant frequency for larger radii provide almost continuous rise in resonant frequency for small inter ring gaps which becomes stable

with increase in gap. Shift in resonant frequency can be achieved up to 7 mm of inter ring gap.

- It will be easy to develop an analytical model for smooth and regular set of data points.
- Design with larger inner radii split ring will provide better selectivity of frequencies for tenability of resonator.

Based on above, rings with larger inner radii (10,11) will provide better results than the smaller radii. Smaller radii provide more shift in resonant frequency but data points are not regular and smooth.

Maximum shift in resonant frequency quantifies the usefulness of dimensional configuration. Maximum shift in resonant frequency can be determined from maximum and minimum values of resonant frequency for a particular option. Two more parameter have been introduced to evaluate specific option for tunability; *usable shift in resonant frequency* and *usable inter ring gap.* Continuously positive shift in resonant frequency will be necessary for design of split ring based tunable resonator. Usable range of inter ring gap can be defined as the maximum value of inter ring gap which will result in continuously positive shift in resonant frequency.

Table 4.1 provides a statistical comparison between various options with different radii of dual broadside coupled split rings with respect to maximum shift in resonant frequency, usable shift in resonant frequency and usable inter ring gap for usable shift in resonant frequency.

TABLE – 4.1: COMPARISON OF SIMULATED DATA FOR SHIFT IN RESONANT FREQUENCY

Positon of lower ring in shield	**Internal radii of split ring (mm)**	**Max shift in resonant frequency (GHz)**	**Usable shift in resonant frequency (GHz)**	**Inter ring gap for usable frequency (mm)**
5 mm above base of shield (Option-II)	8	0.69	039	3
	9	0.63	0.45	3.5
	10	0.65	0.46	4
	11	0.53	0.38	4
	12	0.52	0.28	3
10 mm above base of shield (Option-III)	8	0.79	0.64	5
	9	0.67	0.50	5
	10	0.59	0.39	3
	11	**0.58**	**0.58**	**7.5**
	12	0.52	0.52	5
15 mm above base of shield (Option-IV)	8	0.79	0.40	3
	9	0.78	0.49	4.5
	10	**0.69**	**0.50**	**6.5**
	11	**0.57**	**0.49**	**6**
	12	0.56	0.39	4.5

Table 4.1 also supports the findings inferred from Figure 4.2. Values of usable inter ring gap are very small for Option-II which will reduce the selectivity of the resonator for tunability. Option-III and Option-IV provide much larger range of usable inter ring gap and usable shift in resonant frequency. Hence Option-III and Option-IV with split ring radii of 10 and 11 mm (shown in bold) can be termed as optimized design for tunable split ring resonator based on shift in resonant frequency.

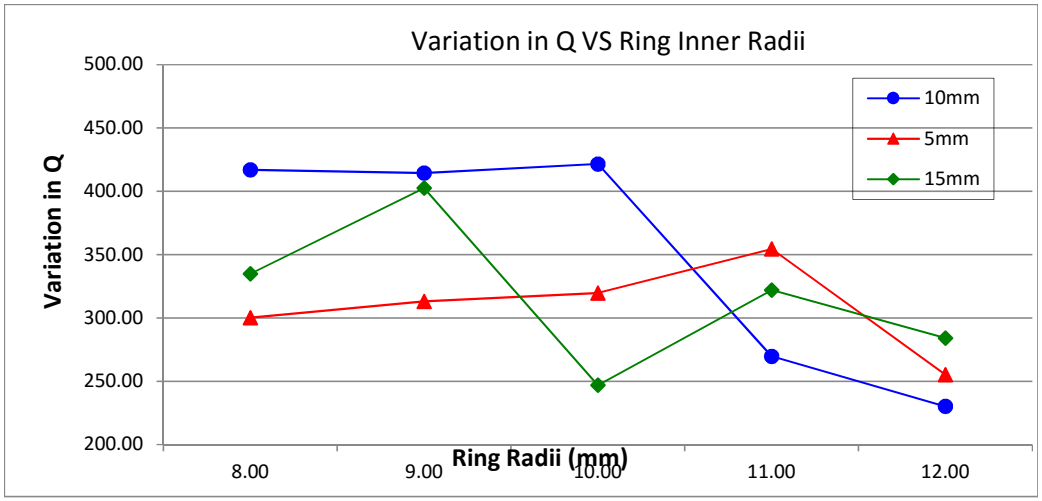

Figure 4.3 – Variation in quality factor at various positions of lower ring with different radii of split rings

4.5 Optimization with respect to Quality Factor

Second important aspect for optimization of broadside coupled split ring resonator configuration is quality factor. Ideally quality factor should remain unchanged throughout this configuration to ensure a fixed bandwidth and selectivity of frequency while tuning the resonator. However, it is not possible due to various factors including coupling, effects of shield and movement of split rings. For best results it is required to select those configurations which offer minimum variations in quality factor over the useful range of inter ring gap.

Options II, III and IV of broadside coupled split rings have been simulated on the lines of resonant frequency. Table 4.2 shows variation in quality factor for each configuration over the useful range of inter ring gap and radii. Variation in quality factor for each configuration is plotted in Figure 4.3 for comparison.

TABLE – 4.2: SIMULATED VARIATION IN QUALITY FACTOR

Internal radii of split ring (mm)	Variation in Quality Factor		
	Lower ring at 5 mm	Lower ring at 10 mm	Lower ring at 15 mm
8	300	417	335
9	313	414	403
10	319	422	247
11	354	270	322
12	355	230	284

Option-II of broadside coupled configuration shows relatively high variation in quality factor. Option II and Option-IV show lesser variation in quality factor for radii of 10 and 11 mm which have already been selected based on shift in resonant frequency.

4.6 Optimized Dimensional Configuration of Dual Broadside Coupled Split Ring Resonator

Optimized dimensional parameters of dual broadside coupled split ring resonator for tunability are tabulated in Table 4.3. Figure 4.4 shows shift in resonant frequency of dual broadside couple split ring resonator based on optimized dimensional parameters.

TABLE – 4.3: OPTIMIZED PARAMETERS FOR DUAL BROADSIDE COUPLED SPLIT RING RESONATOR

	Parameter	Design value
Shield	Inner radius	25~30 mm
	Inner height	30 mm
	Thickness of wall	7 mm
	Material	Aluminum
	Medium inside shield	Air
Split Rings	Height	1 mm

	Parameter	Design value
	Width	1 mm
	Split	1 mm
	Internal radius	10, 11 mm
	Minimum inter ring gap	1 mm
	Max inter ring gap	Up to 7.5 mm
	Material	Copper
	Position of lower split ring	10 mm above base of shield

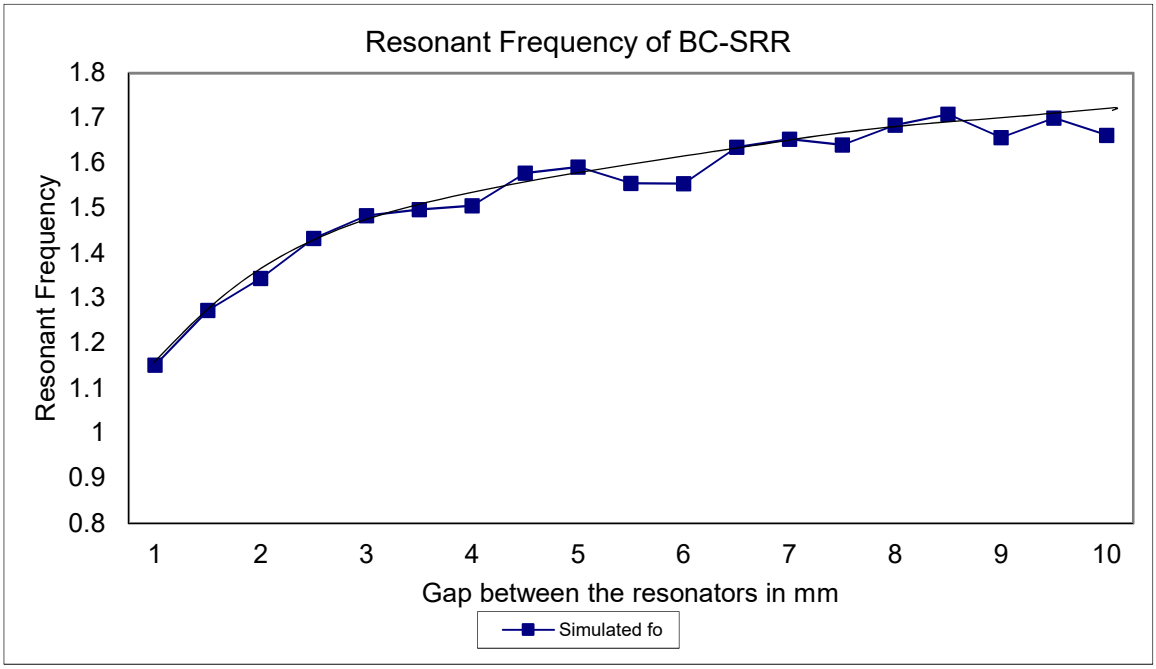

Figure 4.4– Simulated resonant frequency for optimized dual broadside coupled split ring resonator

CHAPTER 5
ANALYTICAL MODEL AND DISCUSSION

ANALYTICAL MODEL AND DISCUSSION

Analytical models have been developed by [9], [10], [12], [16] and [18] to approximate resonant frequency of split ring resonator used for particular application in a particular configuration. Some of these models also give equations to estimate quality factor as well. All these models have been developed for use on single split ring resonators. A comprehensive comparison has been carried out [7]. It has been found that developed analytical models only satisfy a configuration, hence each model needs its own set of equations to estimate resonant frequency and quality factor.

Complementary split ring configuration is being actively used in realization of negative permeability in meta-materials and expressions have been developed to estimate the resonant frequency [20].

5.1 Background

Two main approaches have been used for analytical modeling of split ring based resonators. One of the approach relies on modeling of electric and magnetic fields present inside the shield and split rings; and electric and magnetic energies stored and dissipated. Second approach models split ring resonator as an inductive capacitive (*LC*) resonant network and calculates the resonant frequency using Equation (2.7). Major challenge in this approach is to model the inductive and capacitive elements of split rings. In case of dual broadside coupled split ring resonators, overall inductance and capacitance of *LC* model needs to be estimated.

LC resonant network based model has been used to developed an analytical expression for approximation of resonant frequency of dual broadside coupled split ring resonator configuration. [18] have developed expressions which estimate overall capacitance of a split ring as a combination of surface capacitance and gap capacitance. Equation (2.11) to (2.13) approximate overall capacitance of a single split ring. Self-inductance of split ring is estimated by using formulae [19]. Capacitance of split rings can be added in parallel and average self-inductance of both the rings can be taken as

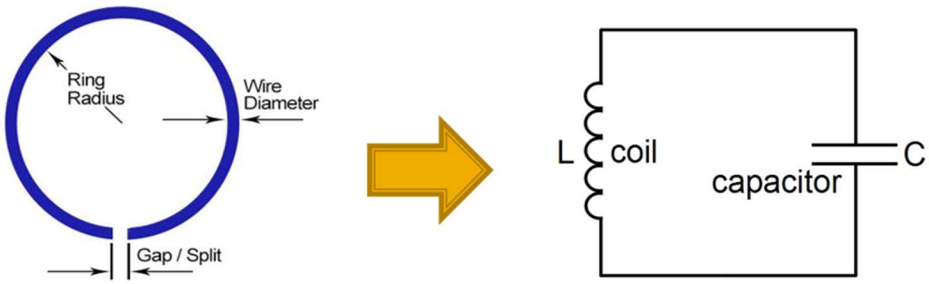

Figure 5.1 – LC resonant network model for single split ring resonator

overall inductance for complementary split rings. Same assumptions can be applied for broadside couple configurations of split rings [20].

5.2 Analytical Model

A single split can be modeled as a *LC resonant network* composed of a one turn inductor and a capacitor. This model is shown in Figure 5.1 where inductance is calculated by Equation (xx) and overall capacitance is calculated by Equation (2.10). This model has been used for development of model for dual broadside coupled split rings configuration.

5.2.1 Assumptions and Basic Model

Following has be assumed for development of analytical model for dual split ring resonators based on previous research:

- Uniform electric and magnetic fields are present inside the shield and split rings. Dimensions of shield are large enough to ensure closed path for magnetic field lines to satisfy the divergence of magnetic flux is zero.
- Resonant frequency of split ring resonators is less than cut off frequency of shield to avoid existence of higher order modes due to shield.
- Fringe effect is considered to extend the uniformity of magnetic and electric field beyond physical dimensions of split rings. Effect of fringed magnetic and electric fields can be approximated by Equation (2.6).

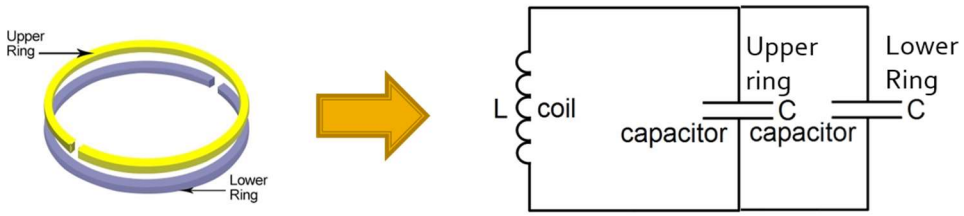

Figure 5.2 – LC resonant network model for dual broadside coupled split rings configuration based on ring capacitances only

- Presence of shield effects the resonant frequency of resonator. Effect of shield on resonant frequency can be approximated.
- Capacitance of both the split rings can be considered in parallel. Overall capacitance will be arithmetic sum of both the capacitances.
- Average value of self-inductance of both the split rings have been used to approximate the overall inductance. Rings have been considered as one turn inductor (split has been neglected).

Based on above assumptions, LC model developed for broadside coupled split rings configuration is shown in Figure 5.2. This model is based on the complementary configuration of split rings which are co-planer Capolino [20].

5.2.2 Proposed Model Based on Inter Ring Capacitance

Another type of capacitance is proposed for dual broadside coupled split rings which is present due to near vicinity of two electrically charged conductors; in this case two split rings. This capacitance can be termed as *coupling capacitance* or *inter ring capacitance*. This capacitance will also be parallel to the other capacitances in already developed model. Figure 5.3 shows modified model of dual broadside coupled split ring resonator. Here C_{inter_ring} is the capacitance between two rings. Total capacitance will be given as under:

$$C_{total} = C_{gap} + C_{surface} + C_{inter\_ring} \tag{5.1}$$

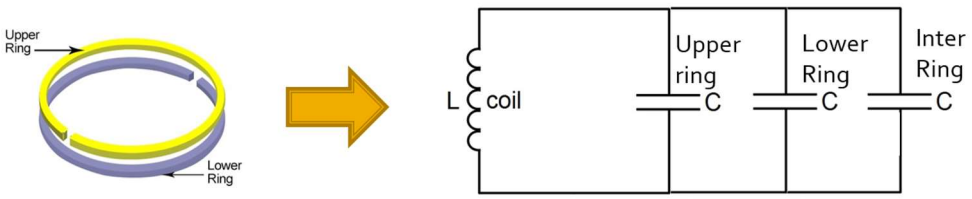

Figure 5.3 – LC resonant network model for dual broadside coupled split rings configuration with proposed inter ring capacitance

This capacitance intuitively should be greater for small inter ring gaps and reduce as inter ring gap increases. This capacitance depends upon inter ring gap. Model of dual broadside couple split rings is shown in Figure 5.3.

5.2.3 Calculation of Inter Ring Capacitance

C_{inter_ring} can be calculated using parallel plate capacitor analogy. Lower face of upper split ring and upper face of lower split rings can be considered as two parallel plates of conducting materials. The gap between the plates is filled with air; which can be considered as dielectric medium. Capacitance between broadside coupled faces of split rings analogous to parallel plate capacitor is given as under:

$$C_{inter\_ring} = \frac{\varepsilon_o \varepsilon_r A}{d} \tag{5.2}$$

where

ε_o is permittivity of free space in Farads/meter

ε_r is relative permittivity of medium (in this case air)

A is the area of parallel faces which contribute capacitor in square meters

d is inter ring gap in meters

One face of split ring is shown in Figure 5.4 for purpose of calculation of area A in Equation 5.2 which constitutes parallel plate capacitor. Area A can be calculated by following expressions:

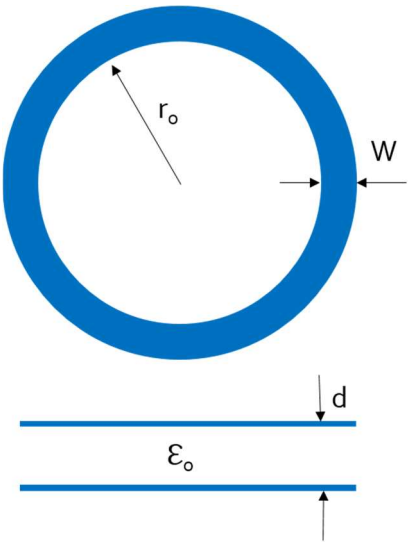

Figure 5.4 – Calculation for inter ring capacitance using parallel plate capacitor model

$$A = \pi((r_o + W)^2 - r_o^2) - (W \times t) \tag{5.3}$$

where

r_o is the internal radius if split ring

W is the width of split ring

t is the width of split

Value of inter ring capacitance can be calculated by substituting value of A from Equation 5.3 into Equation 5.2. Total capacitance has been calculated and tabulated in Table 5.1 for various values of inter ring gap.

TABLE – 5.1: TOTAL CAPACITANCE CALCULATED INCLUDING INTER RING CAPACITANCE

Inter ring gap	**Capacitance (F)**			
(mm)	**gap**	**surface**	**inter_ring**	**Total**
1	3.54167E-14	4.15866E-14	5.75287E-13	7.29E-13
1.5	3.54167E-14	4.15866E-14	3.83525E-13	5.38E-13
2	3.54167E-14	4.15866E-14	2.87644E-13	4.42E-13
2.5	3.54167E-14	4.15866E-14	2.30115E-13	3.84E-13

Inter ring gap (mm)	Capacitance (F)			
	gap	surface	inter_ring	Total
3	3.54167E-14	4.15866E-14	1.91762E-13	3.46E-13
3.5	3.54167E-14	4.15866E-14	1.64368E-13	3.18E-13
4	3.54167E-14	4.15866E-14	1.43822E-13	2.98E-13
4.5	3.54167E-14	4.15866E-14	1.27842E-13	2.82E-13
5	3.54167E-14	4.15866E-14	1.15057E-13	2.69E-13
5.5	3.54167E-14	4.15866E-14	1.04598E-13	2.59E-13
6	3.54167E-14	4.15866E-14	9.58812E-14	2.5E-13
6.5	3.54167E-14	4.15866E-14	8.85057E-14	2.43E-13
7	3.54167E-14	4.15866E-14	8.21839E-14	2.36E-13
7.5	3.54167E-14	4.15866E-14	7.67049E-14	2.31E-13
8	3.54167E-14	4.15866E-14	7.19109E-14	2.26E-13
8.5	3.54167E-14	4.15866E-14	6.76808E-14	2.22E-13
9	3.54167E-14	4.15866E-14	6.39208E-14	2.18E-13
9.5	3.54167E-14	4.15866E-14	6.05565E-14	2.15E-13
10	3.54167E-14	4.15866E-14	5.75287E-14	2.12E-13

Table 5.1 shows values of C_{gap}, $C_{surface}$, C_{inter_ring} and C_{total} for various values of inter ring gap. C_{gap} and $C_{surface}$ are constant as these depend on fixed dimensional parameters of split rings whereas C_{inter_ring} decreases with increase in inter ring gap. Due to the contribution of C_{inter_ring}, C_{total} decrease with increase in inter ring gap. Values shown in Table 5.1 have been plotted in Figure 5.5 which shows fixed and variable capacitances.

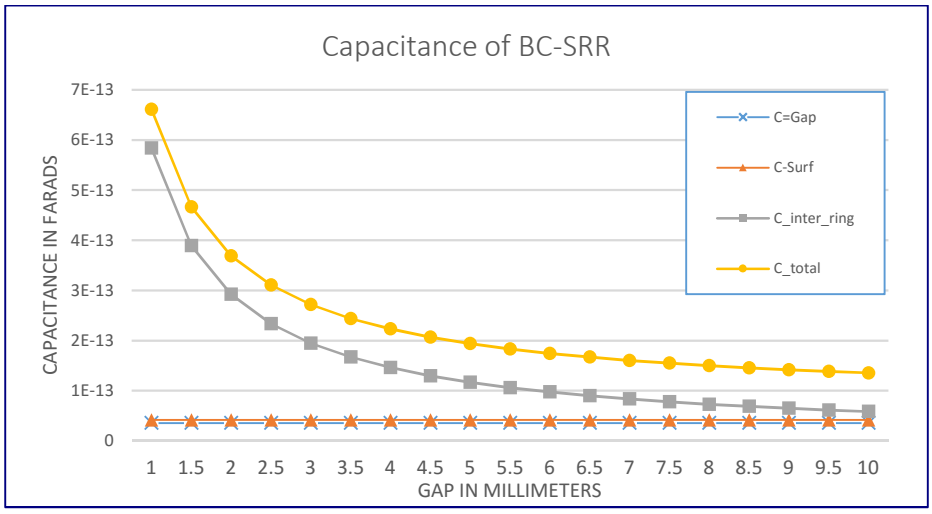

Figure 5.5 – Different types of capacitances of dual broadside coupled split rings

5.3 Comparison of Simulated and Calculated Results

Simulated and calculated resonant frequency for dual broadside coupled split ring resonator is tabulated in Table 5.2 and plotted in Figure 5.6 for comparison and discussion. Calculation are based on the modified expressions for capacitance and existing established expressions for inductance, effect of shield and effect of fringing fields. Calculated values of constants other than the capacitance are as under:

- Average inductance (based on Equation 2.10) = 4.272×10^{-8} H
- Effect of shield (based on part of Equation 2.5) = 1.1902
- Fringe Factor (based on Equations 2.5 and 2.6) = 1.0512

TABLE – 5.2: COMPARISON BETWEEN CALCULATED AND SIMULATED RESUCTS FOR RESONAT FREQUENCY

Inter ring gap (mm)	**Resonant Frequency (GHz)**			**% Difference**
	Calculated	**Simulated**	**Difference**	
1	1.128	1.151	-0.023	-2.03
1.5	1.314	1.273	0.041	3.21
2	1.450	1.344	0.106	7.87

Inter ring gap (mm)	Resonant Frequency (GHz)			% Difference
	Calculated	Simulated	Difference	
2.5	1.554	1.433	0.121	8.45
3	1.638	1.483	0.155	10.46
3.5	1.707	1.447	0.260	17.97
4	1.765	1.505	0.260	17.27
4.5	1.815	1.578	0.237	15.01
5	1.857	1.492	0.366	24.51
5.5	1.895	1.455	0.439	30.17
6	1.927	1.555	0.372	23.94
6.5	1.956	1.636	0.321	19.60
7	1.982	1.653	0.329	19.91
7.5	2.006	1.561	0.445	28.50
8	2.027	1.685	0.342	20.29
8.5	2.046	1.709	0.337	19.74
9	2.064	1.657	0.407	24.54
9.5	2.080	1.700	0.380	22.32
10	2.095	1.462	0.633	43.31

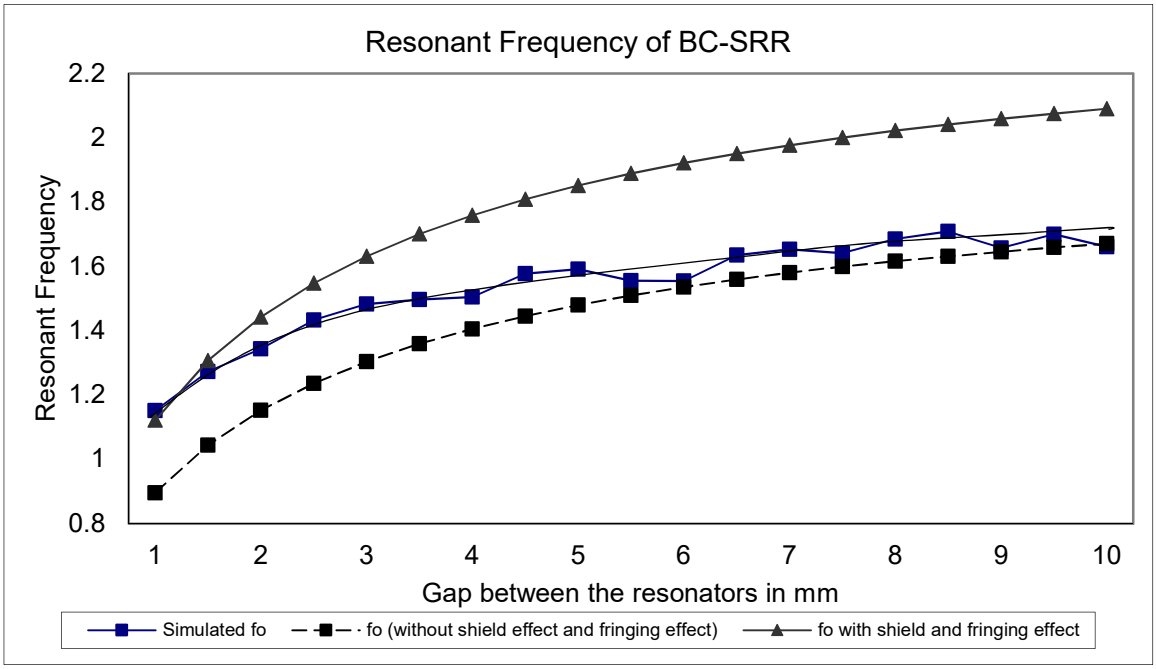

Figure 5.6– Simulated and calculated resonant frequency for optimized dual broadside coupled split ring resonator

5.3.1 Comparison

Comparison of simulated and calculated data gives following:

- Values of resonant frequency calculated from modified expression (including inter ring capacitance) for capacitance generally follow the similar pattern / trend as observed in simulated data.
- Calculated values with shield and fringe effects are closer to simulated values for smaller inter ring gaps which comprises the usable range. This indicates that shield and fringing effects the resonant frequency at smaller inter ring gaps.
- Calculated values without shield and fringe effects are closer to simulated values for larger inter ring gaps. This shows that shield and fringing do not affect the resonant frequency for large inter ring gaps.

- Almost a constant offset can be seen between calculated values and simulated values for values of inter ring gap larger than 5 mm.

5.3.2 Discussion

In this research work a configuration of split ring resonators have been optimized to achieve tunability over a considerable range of frequencies. An optimized design has been presented in Chapter 4. An effort has been made in Chapter 5 to develop an analytical model for the optimized design. *LC* resonant network based analytical model of dual broadside coupled split ring resonator provided results similar to the simulated but not very accurate. In this research, an expression has been developed to calculated the total (overall) capacitance of dual broadside coupled split rings which exhibited its dependence on inter ring gap. The difference between calculated and simulated results can be attributed to the following factors:

- Overall inductance of both the split ring needs to be calculated and its dependence on inter ring gap established.
- Split rings will have varying degree of mutual inductance for varying inter ring gaps. Expression for inductance calculations needs revision.
- Effect of shield is a constant multiple / factor which has been derived for one split ring configuration. Shield will affect the resonant frequency more when the split rings are near to each other due to strengthened magnetic field in the center of split rings and annular region between the split rings and inner surface of shield. This effect will be reduced due to weakened magnetic field of split rings at relatively large inter ring gaps.
- Effect of fringing magnetic fields will be different when split rings are near each other and when placed at relatively greater distance.

Development of analytical model for overall inductance, effect of shield and fringe effect incorporating variable inter ring gap for dual broadside coupled split ring model can increase the accuracy of the calculations.

CHAPTER 6
CONCLUSION AND FUTURE WORK

CONCLUSION AND FUTURE WORK

6.1 Conclusion

Split ring resonators and their use in material characterization and meta-materials are active research area and a lot of studies are underway around the globe. These microwave structure provide a variety of challenges in form of their development, modeling and applications. The initial focus of this research was to find a suitable configuration of split ring based resonator which can provide considerable shift in resonant frequency due to dimensional variation to achieve tunability. Dual broadside coupled split ring configuration was selected and optimized with respect to resonant frequency and quality factor. An approximate analytical model was developed on basis of LC resonant network analogy. A comparison was presented for results from analytical model and simulation; which showed similarities in general and accuracy of 20% within usable range. Proposed method is novel and has not been applied in this scenario before. Utmost effort has been put in to face this multifaceted problem, but it is very difficult to cover all avenues within scope of this study. However, results achieved during this study are very encouraging and promising.

6.2 Future Work

As discussed in earlier sections, main research areas for split ring resonators are material characterization, sensing and meta-materials. Although there is room for improvement in every area mentioned, but especially, a lot of research effort is required for modeling, revision and design of factors mentioned in discussion. This research also provides a jump off point to the field of meta-materials which is most emerging and poses challenges to researchers.

REFERENCES

[1] M. Shoaib, M. Naveed, T. Ejaz, T. Zaidi, M. Amir and M. Ahmad, "Simulation Based Comparative Analysis of Resonant Frequency for Tunable Split Ring Resonator in Different Configurations", in *Fifth International Conference on Advances in Computing, Electronics and Communication - ACEC 2017*, Rome, Italy, 2017, pp. 25-30.

[2] G. B. Collins, *Microwave Magnetron*, New York: McGraw-Hill, 1948, pp. 49-50, 59-62.

[3] Hyde, W. Froncisz and A. Kusumi, "Dispersion electron spin resonance with the loop-gap resonator", *Review of Scientific Instruments*, vol. 53, no. 12, pp. 1934-1937, 1982.

[4] Delayen, G. Dick and J. Mercereau, "Test of a ß ≃ 0.1 superconducting split ring resonator", *IEEE Transactions on Magnetics*, vol. 17, no. 1, pp. 939-942, 1981.

[5] D. Pozar, *Microwave engineering*. Hoboken, NJ: Wiley, 2012, pp. 306-317.

[6] L. F. Chen, C. K. Ong and C. P. Neo, *Microwave Electronics; Measurement and Material Characterization*, 6th ed, Wily, 2004.

[7] T. Ejaz, Rahman, H.U., Shah, S.A.A., and Zaidi, T., "A Comparative Analysis of Split-Ring Resonator Models," in Proceedings of the 4th International Conference on Informatics, Electronics & Vision (ICIEV'15), 2015, p. p. 61.

[8] D. Daly, S. Knight, M. Caulton and R. Ekholdt, "Lumped Elements in Microwave Integrated Circuits", *IEEE Transactions on Microwave Theory and Techniques*, vol. 15, no. 12, pp. 713-721, 1967.

[9] W. Hardy and L. Whitehead, "Split-ring resonator for use in magnetic resonance from 200–2000 MHz", *Review of Scientific Instruments*, vol. 52, no. 2, pp. 213-216, 1981.

[10] W. Froncisz and J. Hyde, "The loop-gap resonator: a new microwave lumped circuit ESR sample structure", *Journal of Magnetic Resonance (1969)*, vol. 47, no. 3, pp. 515-521, 1982.

[11] M. Mehdizadeh, T. Ishii, J. Hyde and W. Froncisz, "Loop-Gap Resonator: A Lumped Mode Microwave Resonant Structure", *IEEE Transactions on Microwave Theory and Techniques*, vol. 31, no. 12, pp. 1059-1064, 1983.

[12] M. Mehdizadeh and T. Ishii, "Electromagnetic field analysis and calculation of the resonance characteristics of the loop-gap resonator", *IEEE Transactions on Microwave Theory and Techniques*, vol. 37, no. 7, pp. 1113-1118, 1989.

[13] Jia-Sheng Hong and M. Lancaster, "Theory and experiment of novel

microstrip slow-wave open-loop resonator filters", *IEEE Transactions on Microwave Theory and Techniques*, vol. 45, no. 12, pp. 2358-2365, 1997.

[14] J. Pendry, A. Holden, D. Robbins and W. Stewart, "Magnetism from conductors and enhanced nonlinear phenomena", *IEEE Transactions on Microwave Theory and Techniques*, vol. 47, no. 11, pp. 2075-2084, 1999.

[15] C. Enkrich, M. Wegener, S. Linden, S. Burger, L. Zschiedrich, F. Schmidt, J. Zhou, T. Koschny and C. Soukoulis, "Magnetic Metamaterials at Telecommunication and Visible Frequencies", *Physical Review Letters*, vol. 95, no. 20, 2005.

[16] S. S. E. a. G. R., Eaton, *Biological Magnetic Resonance: Biomedical EPR, Part B: methodology, instrumentation, and dynamics*, vol. 24, 2005.

[17] A. Masood, A., Castell, O., Barrow, D.A., Allender, C. and Porch, "Split ring resonator technique for compositional analysis of solvents in microcapillary systems," in *The Proceedings of MicroTAS 2008 Conference*, San Diego, 2008 October, pp. pp. 1636-1638.

[18] O. Sydoruk, E. Tatartschuk, E. Shamonina and L. Solymar, "Analytical formulation for the resonant frequency of split rings", *Journal of Applied Physics*, vol. 105, no. 1, p. 014903, 2009.

[19] F. W. Grover, *Inductance Calculations: Working Formulas and Tables*, NC, 1981.

[20] F. Capolino, *Theory and Phenomenon of Metamaterials*, CRC Press, 2009, chapter 16.

[21] C. Balanis, *Advanced Engineering Electromagnetics*, 2nd ed., John Wily and sons, 2012, pp. 227-245.

[22] A. Abduljabar, D. Rowe, A. Porch and D. Barrow, "Novel Microwave Microfluidic Sensor Using a Microstrip Split-Ring Resonator", *IEEE Transactions on Microwave Theory and Techniques*, vol. 62, no. 3, pp. 679-688, 2014.

[23] D. Rowe, S. al-Malki, A. Abduljabar, A. Porch, D. Barrow and C. Allender, "Improved Split-Ring Resonator for Microfluidic Sensing", *IEEE Transactions on Microwave Theory and Techniques*, vol. 62, no. 3, pp. 689-699, 2014.

[24] Ansoft HFSS software version 13. (2017, March) ANSYS HFSS. [Online]. http://www.ansys.com/products/electronics/ansys-hfss

[25] H. Choi, J. Naylon, S. Luzio, J. Beutler, J. Birchall, C. Martin and A. Porch, "Design and In Vitro Interference Test of Microwave Noninvasive Blood Glucose Monitoring Sensor", *IEEE Transactions on Microwave Theory and Techniques*, vol. 63, no. 10, pp. 3016-3025, 2015.

[26] M. Wellenzohn and M. Brandl, "A Theoretical Design of a Biosensor Device Based on Split Ring Resonators for Operation in the Microwave Regime", *Procedia Engineering*, vol. 120, pp. 865-869, 2015.

[27] Xutao Tang, Iryna E. Khodasevych, and Wayne S. T. Rowe, "Tunable split ring resonators using air pressure," in *Microwave Symposium (AMS), 2016 IEEE 2nd Australian*, 2016.

[28] T., Ejaz, T., Naveed, M., Zaidi, T. and Rahman, H.U. Hayat, "Simulation Based Comparative Analysis of Split Resonators for Compositional Analysis.," in *The Fourth International Conference on Technological Advances in Electrical, Electronics*, 2016, September.

[29] T. Ejaz, H. Ur Rahman, T. Tauqeer, A. Masood and T. Zaidi, "Shield Optimization and Formulation of Regression Equations for Split-Ring Resonator", *Mathematical Problems in Engineering*, vol. 2016, pp. 1-10, 2016.

[30] R. Alahnomi, Z. Zakaria, E. Ruslan, A. Azuan, M. Bahar, "A Novel Symmetrical Split Ring Resonator Based on Microstrip for Microwave Sensors," *Measurement Science Review,* vol. 16, no. 1, pp. 21-27, 2016.